Theor. Comput. Fluid Dyn. (2007) 21: 99–118
DOI 10.1007/s00162-006-0036-8

ORIGINAL ARTICLE

Stefan Heinz

Unified turbulence models for LES and RANS, FDF and PDF simulations

Received: 30 September 2005 / Accepted: 18 July 2006 / Published online: 6 September 2006

Abstract A review of existing basic turbulence modeling approaches reveals the need for the development of unified turbulence models which can be used continuously as filter density function (FDF) or probability density function (PDF) methods, large eddy simulation (LES) or Reynolds-averaged Navier–Stokes (RANS) methods. It is then shown that such unified stochastic and deterministic turbulence models can be constructed by explaining the dependence of the characteristic time scale of velocity fluctuations on the scale considered. The unified stochastic model obtained generalizes usually applied FDF and PDF models. The unified deterministic turbulence model that is implied by the stochastic model recovers and extends well-known linear and nonlinear LES and RANS models for the subgrid-scale and Reynolds stress tensor.

Keywords Filter density function · Probability density function · Large eddy simulation · Reynolds-averaged Navier–Stokes equations · Unified turbulence models

PACS 47.11.−j, 47.27.E−, 47.27.eb

1 Introduction

The numerical integration of the basic equations of fluid and thermodynamics represents a unique tool for studying fundamental mechanisms of turbulent flows, but the computational costs related to such direct numerical simulation (DNS) do not allow applications to most engineering and environmental flows [1–5]. In order to overcome this problem one has to reduce the computational requirements by modeling at least a part of the spectrum of turbulent motions. Such turbulence modeling can be performed in two basic ways. The first way applies modeling assumptions to processes at all scales, which results in deterministic Reynolds-averaged Navier–Stokes (RANS) [4, 6–8] or stochastic probability density function (PDF) methods [4, 9–13]. The second way applies modeling assumptions to small-scale processes, which results in deterministic large eddy simulation (LES) [4, 14–18] or stochastic filter density function (FDF) methods [12, 19–27]. It is worth noting that PDF and FDF methods overcome closure problems of RANS and LES equations by explaining the dynamics of fluctuations (so that reacting flows can be treated without the need to close filtered reaction rates). There are also several intermediate strategies, e.g., very large eddy simulation (VLES), unsteady RANS (URANS) and detached eddy simulation (DES) methods [28–30].

The availability of unified turbulence models that could be used continuously to perform LES and RANS, FDF and PDF simulations appears to be very helpful for a better understanding of the generality of modeling assumptions, and to make optimal use of the characteristic advantages of models. Nevertheless, existing models do not represent unified turbulence models [12, 17, 28, 30, 31]. The question of how it is possible to develop

Communicated by S. Obi.

S. Heinz
Department of Mathematics, University of Wyoming, 1000 East University Avenue, Laramie, WY 82071, USA
E-mail: heinz@uwyo.edu

such unified turbulence models will be addressed here. To provide a basis for the following developments and to explain the basic techniques applied, the fluid dynamic equations that are implied by molecular motion will be presented in Sect. 2. The rescaling of these equations allows the construction of stochastic and deterministic turbulence models. This will be shown in Sects. 3 and 4 with regard to PDF/RANS and FDF/LES equations, respectively. The questions of why it is needed and how it is possible to develop unified models for compressible turbulent flows is considered in Sect. 5. Conclusions of this analysis are presented in Sect. 6.

2 The fluid dynamics implied by molecular motion

First, let us consider the modeling of fluid dynamics at the molecular scale. In Sects. 3 and 4 the analogy between molecular and turbulent motion [32, 33] will then be used for the construction of equations for turbulent motion. The following discussion also includes an explanation of the methodologies used to derive the deterministic equations and the related algebraic closure models from the underlying stochastic equations.

2.1 The fluid dynamic variables

Fluid dynamic variables can be defined on the basis of conditional ensemble means. We define the mean of any function Q of molecular properties (for example, velocities) conditioned on the position $\mathbf{x} = (\mathrm{x}_1, \mathrm{x}_2, \mathrm{x}_3)$ in physical space by

$$\bar{Q}(\mathbf{x}, t) = \frac{1}{\rho(\mathbf{x}, t)} \langle \rho_{\mathrm{m}}(\mathbf{x}, t)\, Q \rangle. \tag{2.1}$$

The symbol $\langle \cdots \rangle$ denotes an ensemble mean. By setting $Q = 1$ in (2.1) one observes that the mean mass density $\rho(\mathbf{x}, t)$ represents the ensemble mean of ρ_{m}, this means $\rho(\mathbf{x}, t) = <\rho_{\mathrm{m}}(\mathbf{x}, t)>$. The instantaneous molecular mass density ρ_{m} is defined by

$$\rho_{\mathrm{m}}(\mathbf{x}, t) = M\, \delta\big(\mathbf{x}^*(t) - \mathbf{x}\big). \tag{2.2}$$

Here, δ refers to the delta function and $\mathbf{x}^*(t) = (x_1^*, x_2^*, x_3^*)$ is the position of a molecule at time t. The spatial integration of (2.2) reveals that M represents the total mass of molecules within the domain considered.

By invoking the ergodic theorem [34], the ensemble averaging considered may be seen as a filtering in space where the filter width is much smaller than the domain considered but so large that a very large number of molecules is involved in the calculation of means at $\mathbf{x}$. Such ensemble-averaged variables describe, therefore, the properties of a continuum: they represent fluid dynamic variables, such as for instance the fluid mass density or velocity.

The density-weighted mean (2.1) may also be represented as the mean of a PDF. This relation reads

$$\bar{Q}(\mathbf{x}, t) = \int \mathrm{d}\mathbf{w}\; Q(\mathbf{w}, \mathbf{x}, t)\, F(\mathbf{w}, \mathbf{x}, t), \tag{2.3}$$

where the conditional PDF of the molecular velocities is given by

$$F(\mathbf{w}, \mathbf{x}, t) = \frac{1}{\rho(\mathbf{x}, t)} \big\langle \rho_{\mathrm{m}}(\mathbf{x}, t)\, \delta\big(\boldsymbol{V}^*\big(\mathbf{x}^*(t), t\big) - \mathbf{w}\big) \big\rangle. \tag{2.4}$$

Here, $\boldsymbol{V}^*(\mathbf{x}^*(t), t) = (V_1^*, V_2^*, V_3^*)$ is the velocity of a molecule. To show the consistency of $\bar{Q}$ definitions one has to apply (2.4) in (2.3). The use of the shifting property of delta functions and integration over the velocity sample space then recovers the $\bar{Q}$ definition (2.1).

According to (2.3), fluid dynamic variables in addition to the mass density $\rho(\mathbf{x}, t) = \langle \rho_{\mathrm{m}}(\mathbf{x}, t) \rangle$ may be obtained from F by multiplying it by the corresponding variables and integrating over the sample space. The mean velocity U_i $(i = 1, 3)$ of molecules

$$U_i(\mathbf{x}, t) = \int \mathrm{d}\mathbf{w}\, F(\mathbf{w}, \mathbf{x}, t)\, w_i \tag{2.5}$$

describes the fluid velocity at time t in an infinitesimal vicinity of $\mathbf{x}$. The variance of F is characterized by the molecular stress tensor M_{ij}, which is given by

$$M_{ij} = \int \mathrm{d}\mathbf{w}\ F(\mathbf{w}, \mathbf{x}, t)(w_i - U_i)\big(w_j - U_j\big). \tag{2.6}$$

Regarding the following developments it is helpful to write M_{ij} in terms of isotropic and deviatoric contributions,

$$M_{ij} = 2e\left[\frac{1}{3}\delta_{ij} + m_{ij}\right]. \tag{2.7}$$

Here, $e = M_{kk}/2$ represents the specific kinetic energy e of molecular velocity fluctuations (the sum convention is applied throughout this paper) and $m_{ij} = (M_{ij} - M_{kk}\delta_{ij}/3)/(2e)$ is the standardized deviatoric molecular stress tensor. Further moments of F are given correspondingly. For example,

$$T_{ijk} = \int \mathrm{d}\mathbf{w}\ F(\mathbf{w}, \mathbf{x}, t)(w_i - U_i)\big(w_j - U_j\big)(w_k - U_k) \tag{2.8}$$

is the molecular triple correlation tensor that appears in the molecular stress transport equation (see Sect. 2.3).

2.2 Stochastic equations

To calculate the PDF F, one needs a model for the molecular positions $\mathbf{x}^*(t)$ and velocities $\mathbf{V}^*(t)$. Such microscale modeling of thermal fluctuations is usually addressed on the basis of the Boltzmann equation. However, the derivation of fluid dynamic equations in this way is problematic [35–37]. The first problem arises from the fact that the construction of the Boltzmann equation is related to the consideration of rarefied gases, whereas one is interested in dense fluids (gases and liquids) in fluid mechanics in general. The second problem is related to the fact that the derivation of extensions to the Navier–Stokes model poses a nontrivial problem. By adopting this approach one may find various equations, and the physical relevance of such extensions to the Navier–Stokes model is not clarified [37–40].

A way to overcome these problems is to construct stochastic equations for molecular motion. By adopting a systematic projection method [12, 41–42] one may extract an equation for the motion of one molecule from known equations for the coupled motion of all molecules. This approach explains molecular dynamics by a interaction of the molecule considered with the collective of all the other molecules: the molecule considered is accelerated due to random impacts of other molecules and decelerated because other molecules damp its motion. By neglecting possible contributions due to external forces, one obtains in this way for the molecular positions x_i^* and velocities V_i^* ($i = 1, 3$) the equations [42]

$$\frac{\mathrm{d}x_i^*}{\mathrm{d}t} = V_i^*, \tag{2.9a}$$

$$\frac{\mathrm{d}V_i^*}{\mathrm{d}t} = -\frac{1}{\tau_\mathrm{m}}\big(V_i^* - U_i\big) + \sqrt{\frac{4e}{3\tau_\mathrm{m}}}\frac{\mathrm{d}W_i}{\mathrm{d}t}. \tag{2.9b}$$

The right-hand side of (2.9b) explains the mechanism of molecular velocity fluctuations as a competition between the generation of fluctuations and their relaxation. The generation of fluctuations is described by the noise term (the last term), which is determined by the properties of $\mathrm{d}W_\mathrm{i}/\mathrm{d}t$. The latter is a Gaussian process with vanishing means, $\langle \mathrm{d}W_i/\mathrm{d}t\rangle = 0$, and uncorrelated values at different times, $\langle \mathrm{d}W_i/\mathrm{d}t(t) \cdot \mathrm{d}W_j/\mathrm{d}t'(t')\rangle = \delta_{ij}\delta(t - t')$. The symbol δ_{ij} is the Kronecker delta. The specific kinetic energy $e = M_{kk}/2$ of molecular velocity fluctuations controls the intensity of fluctuations. The relaxation of fluctuations is described by the first term on the right-hand side of (2.9b): V_i^* relaxes towards the fluid velocity U_i where τ_m characterizes the relaxation time scale of velocity fluctuations. The noise strength $4e/(3\tau_\mathrm{m})$ and molecular relaxation frequency τ_m^{-1} are given in (2.9b) by isotropic quantities. The latter assumption corresponds to the idea that there are isotropic random impacts of other molecules and a corresponding isotropic relaxation of molecular velocity fluctuations only in interaction with their mean velocity U_i.

2.3 Deterministic equations

All molecular statistics can be obtained by solving (2.9a,b) directly. However, such a Monte Carlo simulation turns out to be much too expensive to calculate most flows. A way to reduce the computational costs is to simply (2.9a,b) to deterministic equations. To do this we rewrite the model (2.9a,b) as a Fokker–Planck equation for the molecular velocity PDF $F(\mathbf{w}, \mathbf{x}, t)$. This PDF equation reads [12, 42]

$$\frac{\partial \rho F}{\partial t} + \frac{\partial \rho w_k F}{\partial x_k} = \frac{1}{\tau_\mathrm{m}} \frac{\partial}{\partial w_i} \left[w_i - U_i + \frac{2}{3} e \frac{\partial}{\partial w_i} \right] \rho F. \tag{2.10}$$

By multiplying (2.10) by 1, w_i and w_i, w_j, respectively, and integrating the resulting equations over the velocity sample space, one may derive the following compressible flow transport equations for the fluid mass density $\rho(\mathbf{x}, t)$, the velocity U_i and the molecular stress tensor M_{ij}:

$$\frac{\mathrm{D}\rho}{\mathrm{D}t} = -\rho \frac{\partial U_k}{\partial x_k}, \tag{2.11a}$$

$$\frac{\mathrm{D}U_i}{\mathrm{D}t} + \frac{1}{\rho} \frac{\partial \rho M_{ik}}{\partial x_k} = 0, \tag{2.11b}$$

$$\frac{\mathrm{D}M_{ij}}{\mathrm{D}t} + \frac{1}{\rho} \frac{\partial \rho T_{kij}}{\partial x_k} + M_{ik} \frac{\partial U_j}{\partial x_k} + M_{jk} \frac{\partial U_i}{\partial x_k} = -\frac{2}{\tau_\mathrm{m}} \left(M_{ij} - \frac{2}{3} e \delta_{ij} \right). \tag{2.11c}$$

Here, $\mathrm{D}/\mathrm{D}t = \partial/\partial t + U_k \, \partial/\partial x_k$ denotes the Lagrangian time derivative along the fluid velocity field, and T_{ijk} is the triple correlation tensor defined by (2.8).

Equation (2.11c) can be used to calculate an algebraic expression for the molecular stress tensor $M_{ij} = 2e(\delta_{ij}/3 + m_{ij})$, which can be used for the closure of Eq. (2.11b). To do this it is helpful to rewrite (2.11c) as an equation for the standardized deviatoric molecular stress tensor m_{ij} and an equation for e. These equations read

$$\frac{\mathrm{D}e}{\mathrm{D}t} + \frac{1}{2\rho} \frac{\partial \rho T_{knn}}{\partial x_k} + 2e \left(m_{nk} + \frac{1}{3} \delta_{nk} \right) \frac{\partial U_n}{\partial x_k} = 0, \tag{2.12a}$$

$$\frac{\mathrm{D}m_{ij}}{\mathrm{D}t} + \frac{1}{2\rho e} \frac{\partial \rho (T_{kij} - T_{knn}\delta_{ij}/3)}{\partial x_k} + \frac{m_{ij}}{e} \frac{\mathrm{D}e}{\mathrm{D}t} + m_{ik} \frac{\partial U_j}{\partial x_k} + m_{jk} \frac{\partial U_i}{\partial x_k} - \frac{2}{3} m_{nk} \frac{\partial U_n}{\partial x_k} \delta_{ij} = -\frac{2}{\tau_\mathrm{m}} m_{ij} - \frac{2}{3} S^d_{ij}. \tag{2.12b}$$

$S^d_{ij} = S_{ij} - S_{nn}\delta_{ij}/3$ is the deviatoric part of the rate-of-strain tensor $S_{ij} = (\partial U_i/\partial x_j + \partial U_j/\partial x_i)/2$. Equation (2.12b) can be used for the calculation of m_{ij} in the following way [42]. In the first order of approximation, we neglect all transport terms (the first three terms on the left-hand side) and production terms (the last three terms on the left-hand side) of Eq. (2.12b). Correspondingly, one finds $m^{(1)}_{ij} = -\tau_\mathrm{m} S^d_{ij}/3$ in this first-order approximation. This implies the Navier–Stokes model

$$M^{(1)}_{ij} = \frac{2}{3} e \delta_{ij} - 2\nu \, S^d_{ij}. \tag{2.13}$$

Here, the kinematic viscosity $\nu = e\tau_\mathrm{m}/3$ is introduced such that the molecular time scale is given by

$$\tau_\mathrm{m} = 3\nu/e. \tag{2.14}$$

The second order of approximation for M_ij is given by neglecting [in consistency with the assumption of isotropic coefficients $4e/(3\tau_\mathrm{m})$ and τ_m^{-1} in (2.9b)] the deviatoric triple correlation contribution and adopting the first-order approximation for M_{ij} in all the other expressions of the left-hand side of (2.12b). According to (2.12a) we apply $\mathrm{D}e/\mathrm{D}t = -2S_\mathrm{nn}e/3$ (note that $m_{nk}\partial U_n/\partial x_k$ represents a term of higher order). Correspondingly, we find the following second order of approximation for the molecular stress tensor M_{ij}:

$$M^{(2)}_{ij} = \frac{2}{3} e \delta_{ij} - 2\nu \left(S^d_{ij} - \frac{1}{2} \frac{D \tau_\mathrm{m} S^d_{ij}}{Dt} \right) + \frac{3\nu^2}{e} \left[2 S^d_{ik} S^d_{kj} - \frac{2}{3} S^d_{nk} S^d_{kn} \, \delta_{ij} - S^d_{ik} \Omega_{kj} - S^d_{jk} \Omega_{ki} \right]. \tag{2.15}$$

Here, $\Omega_{ij} = (\partial U_i/\partial x_j - \partial U_j/\partial x_i)/2$ is the rate-of-rotation tensor. An analysis of the scaling of $M_{ij}^{(2)}$ reveals that terms in addition to $M_{ij}^{(1)}$ scale with the squared Knudsen number Kn [42], which is very small for flows with a relatively small Mach number and a relatively high Reynolds number. Under these conditions (which are given for most of the flows of practical relevance), it is well justified to use the first-order approximation $M_{ij}^{(1)}$. The turbulence models described in Sects. 3, 4 and 5 will be presented for such flows governed by the compressible Navier–Stokes equations (which are given by combining (2.11a,b) with (2.13) for M_{ij}).

2.4 The BGK model

It is of interest to compare the nonlinear molecular stress model (2.15) with consequences of other kinetic equations. To do this, let us consider a modified Boltzmann equation given by the Bhatnagar, Gross and Krook (BGK) model [43]

$$\frac{\partial \rho F}{\partial t} + \frac{\partial \rho w_k F}{\partial x_k} = -\frac{2\rho}{\tau_{\mathrm{m}}}\left(F - F_{\mathrm{eq}}\right). \tag{2.16}$$

The PDF F evolves towards its equilibrium PDF F_{eq}, which is modeled as an isotropic Gaussian PDF,

$$F_{\mathrm{eq}} = \frac{1}{(4\pi e/3)^{3/2}} \exp\left\{-\frac{(w_i - U_i)(w_i - U_i)}{4e/3}\right\}. \tag{2.17}$$

The implied transport equations for the fluid mass density $\rho(\mathbf{x}, t)$, velocity U_i and stress tensor M_{ij} are again given by (2.11a–c). The use of the procedure described above shows that the nonlinear molecular stress model obtained on the basis of the BGK model is again given by (2.15). It is of interest to note that the same nonlinear stress model can be derived from the stress transport equation by adopting the Chapman–Enskog expansion technique, which accounts for small deviations of F from the equilibrium PDF F_{eq} [33]. The latter fact provides additional support for the validity of the nonlinear stress model (2.15). Compared to the use of invariance constraints for the construction of nonlinear stress models [44], an important advantage of using stress models derived from kinetic equations is given by the fact that all the model coefficients are obtained consistently.

Regarding the differences between the stochastic model (2.9a,b) and the BGK model (2.16) it is worth emphasizing that the rescaling of (2.16) for turbulent flow computations suffers from significant problems. It is impossible to account correctly for the transport of mean velocities in inhomogeneous turbulent flows, such that the range of applicability of such a model would be limited to homogeneous flows. The turbulent kinetic energy equation implied by a BGK model for turbulent flow does not involve dissipation of turbulent kinetic energy. To overcome this problem one could modify the variance in the equilibrium PDF F_{eq} by a nondimensional factor such that the stress transport equation implied by the BGK model would correspond to Eq. (3.6c). However, for the case of homogeneous turbulence, one finds that such a BGK model does not allow an asymptotic Gaussian solution. The comparison with experimental data then reveals that such a model behavior disagrees with observations [45]. Due to these reasons, the BGK model does not provide a basis for the development of models for turbulent motion.

3 Large-scale turbulence modeling

The microscale Eqs. (2.11a,b) combined with a molecular stress tensor model are applicable to simulate macroscale processes, but such an application of DNS is much too expensive to calculate most turbulent flows of practical relevance. Thus, there is a need to develop equations that do not involve all the details of molecular motion. Depending on the type of filtering applied, such turbulence modeling can be performed in two basic ways: one can apply PDF/RANS methods involving ensemble-averaged variables, or one can apply FDF/LES methods involving spatially filtered variables. Essential features of PDF/RANS methods will be described in this section. Their advantages and disadvantages will be discussed in comparison with FDF/LES methods in Sect. 5.1. According to the discussion following relation (2.15), these methods will be presented with regard to flows that can be described by the compressible Navier–Stokes equations.

3.1 Ensemble-averaged variables

One approach to develop equations for macroscale processes is to consider (in correspondence to the development of molecular equations) the dynamics of ensemble-averaged variables. Such mass-density-weighted ensemble-averaged variables can be defined by

$$\bar{Q}(\mathbf{x}, t) = \frac{1}{\langle \rho(\mathbf{x}, t) \rangle} \langle \rho(\mathbf{x}, t)\, Q \rangle, \tag{3.1}$$

where Q refers to any variable that fluctuates on the fluid dynamic scale. The symbol $\langle \cdots \rangle$ denotes an ensemble mean, and $\rho(\mathbf{x}, t)$ represents the instantaneous fluid mass density.

However, a significant problem of using ensemble-averaged variables is the following. According to the ergodic hypothesis [34], ensemble-averaged fluid dynamic variables may be seen as spatial averages where the filter width is large compared to the characteristic length scale of turbulent eddies. In other words, all the spectrum of turbulent motions has to be modeled by developing equations for the dynamics of ensemble-averaged fluid dynamic variables.

3.2 Stochastic equations

In correspondence to the presentation of equations for molecular motion, let us first consider stochastic equations for turbulent motion. This approach allows the derivation of closure models for correlations of turbulent fluctuations that appear as unknowns in deterministic equations. A particular advantage is given by the fact that the realizability (the constraint that any transport equations for correlations of turbulent fluctuations should represent realizable equations for correlations of a stochastic process) of closure models is assured in this way. Realizability was proven to represent a valuable guiding principle for turbulence modeling [46–49]. Correspondingly, the use of realizable closure models was found to be of remarkable relevance regarding the application of PDF and RANS methods [50–52].

The stochastic model considered is the generalized Langevin model for the ith components of fluid particle positions x_i^* and velocities U_i^*. This PDF model for compressible flow reads [4, 9–12]

$$\frac{\mathrm{d}}{\mathrm{d}t} x_i^* = U_i^*, \tag{3.2a}$$

$$\frac{\mathrm{d}}{\mathrm{d}t} U_i^* = \frac{2}{\langle \rho \rangle} \frac{\partial \langle \rho \rangle \bar{\nu}\, \bar{S}_{ik}^d}{\partial x_k} - \frac{1}{\langle \rho \rangle} \frac{\partial \langle p \rangle}{\partial x_i} + G_{ij} \left(U_j^* - \bar{U}_j \right) + \sqrt{\frac{4 c_0^{(PDF)} k}{3 \tau_L^{(PDF)}}} \frac{\mathrm{d}W_\mathrm{i}}{\mathrm{d}t}. \tag{3.2b}$$

The analogy between equations for molecular and turbulent motion [32–33] provides the basis for this model. First of all, fluctuations are characterized by their energy and characteristic relaxation time. To adopt the molecular equations (2.9a,b) for the modeling of turbulent motions, one has to replace, therefore, the molecular energy e of fluctuations and relaxation time scale τ_m by the turbulent kinetic energy k and relaxation time scale $\tau_L^{(\mathrm{PDF})}$ used in PDF methods for turbulent flows.

The comparison between (3.2b) and (2.9b) shows that Eq. (3.2b) is more general than Eq. (2.9b). A first difference is given by the inclusion of spatial transport terms [the first two terms on the right-hand side of Eq. (3.2b)]. These terms involve the averaged mass density $\langle \rho \rangle$, viscosity $\bar{\nu}$, deviatoric rate-of-strain tensor $\bar{S}_{ik}^d$ (for simplicity, ν and S_{ij}^d are assumed to be uncorrelated), and pressure $\langle p \rangle$. Equation (3.6b) given in Sect. 3.3 reveals the need to include these spatial gradient terms: these terms assure the correct transport of mean velocities. A second difference between (3.2b) and (2.9b) is given by the consideration of an anisotropic matrix G_{ij}. As shown in Sects. 3.3 and 3.4, such an anisotropic matrix G_{ij} has to be considered in order to account correctly for the anisotropy of the Reynolds stress tensor. In analogy to (2.9b) we define a characteristic relaxation time scale $\tau_L^{(\mathrm{PDF})} = -3/G_{nn}$. A third difference to (2.9b) is given by the consideration of $c_0^{(\mathrm{PDF})}$ in (3.2b). The need to involve this nondimensional parameter [which is equal to 1 in (2.9b)] may be seen by looking at Eq. (3.7a). The right-hand side of this equation represents the negative dissipation rate ϵ of turbulent kinetic energy, this means

$$\varepsilon = 2 \left(1 - c_0^{(\mathrm{PDF})} \right) k / \tau_L^{(\mathrm{PDF})}. \tag{3.3}$$

Consequently, the assumption $c_0^{(\mathrm{PDF})} = 1$ would incorrectly imply that the dissipation of turbulent kinetic energy is zero (fluid particles do not conserve kinetic energy as molecules).

The Eqs. (3.2a,b) are unclosed as long as the time scale $\tau_L^{(\mathrm{PDF})}$ of turbulent motion is not defined. By Eq. (3.3), this time scale is given by

$$\tau_L^{(\mathrm{PDF})} = 2\left(1 - c_0^{(\mathrm{PDF})}\right) L\, k^{-1/2}. \tag{3.4}$$

Here, $L = k^{3/2}/\epsilon$ is the characteristic length scale of large-scale turbulent eddies. No assumptions are made regarding the calculation of L. This length scale can be provided by a variety of methods [4, 7] which may well involve several relevant length or time scales [53]. By adopting (3.4), the noise term in Eq. (3.2b) may be written in terms of its standard formulation $(C_0^{(\mathrm{PDF})}\varepsilon)^{1/2}\mathrm{d}W_i/\mathrm{d}t$. Here, $C_0^{(\mathrm{PDF})} = 2c_0^{(\mathrm{PDF})}/\left[3(1 - c_0^{(\mathrm{PDF})})\right]$ refers to the Kolmogorov constant for high-Reynolds-number turbulence. By rewriting this expression for $C_0^{(\mathrm{PDF})}$ we obtain for the calculation of $c_0^{(\mathrm{PDF})}$ the relation

$$c_0^{(\mathrm{PDF})} = \frac{C_0^{(\mathrm{PDF})}}{C_0^{(\mathrm{PDF})} + 2/3}. \tag{3.5}$$

This relation reveals that $c_0^{(\mathrm{PDF})}$ is bounded ($0 \le c_0^{(\mathrm{PDF})} \le 1$) because $C_0^{(\mathrm{PDF})} \ge 0$. Expression (3.5) can be used to calculate $c_0^{(\mathrm{PDF})}$ by adopting available $C_0^{(\mathrm{PDF})}$ measurements. As discussed in detail elsewhere [54] one finds for structured flows (decaying turbulence, evolving scalar fields, the atmospheric boundary layer and channel flows) $C_0^{(\mathrm{PDF})}$ values near two if accurate models are applied. Higher $C_0^{(\mathrm{PDF})}$ values near six are found for less-structured flows (homogeneous, isotropic, stationary turbulence) or models that involve simplifying assumptions. The reason for these differences is given by the fact that additional stochastic forcing is needed to compensate for the disappearance or neglect of contributions due to acceleration fluctuations or anisotropic turbulence [54]. These $C_0^{(\mathrm{PDF})}$ variations imply a range $c_0^{(\mathrm{PDF})} = 0.83 \pm 0.07$ of $c_0^{(\mathrm{PDF})}$ variations.

3.3 Deterministic equations

The generalized Langevin model (3.2a,b) can be used to derive deterministic equations (which require less computational costs) for the transport of mean variables. The way to obtain these equations was explained above with regard to molecular motion. By rewriting (3.2a,b) as the corresponding Fokker–Planck equation for the PDF, one obtains the following RANS equations for the mean mass density $\langle\rho\rangle$, mass-density-weighted velocity $\tilde{U}_i$, and Reynolds stresses R_{ij} (the variance of the velocity PDF: $R_{ij} = \overline{u_i u_j}$, where u_i refers to turbulent velocity fluctuations):

$$\frac{\tilde{\mathrm{D}}\langle\rho\rangle}{\tilde{\mathrm{D}}t} = -\langle\rho\rangle\frac{\partial\tilde{U}_k}{\partial x_k}, \tag{3.6a}$$

$$\frac{\tilde{\mathrm{D}}\,\tilde{U}_i}{\tilde{\mathrm{D}}t} + \frac{1}{\langle\rho\rangle}\frac{\partial\langle\rho\rangle R_{ik}}{\partial x_k} = \frac{2}{\langle\rho\rangle}\frac{\partial\langle\rho\rangle\bar{\nu}\,\tilde{S}_{ik}^d}{\partial x_k} - \frac{1}{\langle\rho\rangle}\frac{\partial\langle p\rangle}{\partial x_i}, \tag{3.6b}$$

$$\frac{\tilde{\mathrm{D}}R_{ij}}{\tilde{\mathrm{D}}t} + \frac{1}{\langle\rho\rangle}\frac{\partial\langle\rho\rangle T_{kij}^R}{\partial x_k} + R_{ik}\left(\frac{\partial\tilde{U}_j}{\partial x_k} - G_{jk}\right) + R_{jk}\left(\frac{\partial\tilde{U}_i}{\partial x_k} - G_{ik}\right) = \frac{4c_0^{(\mathrm{PDF})}k}{3\tau_L^{(\mathrm{PDF})}}\delta_{ij}. \tag{3.6c}$$

$\tilde{\mathrm{D}}/\tilde{\mathrm{D}}t = \partial/\partial t + \tilde{U}_k\,\partial/\partial x_k$ refers to the mean Lagrangian time derivative, and T_{kij}^R represents the triple correlation tensor of velocity fluctuations [corresponding to the T_{ijk} defined by relation (2.8): $T_{kij}^R = \overline{u_i u_j u_k}$]. Equation (3.6c) for the Reynolds stress tensor $R_{ij} = 2k(\delta_{ij}/3 + r_{ij})$ can be rewritten in terms of equations for

the turbulent kinetic energy $k = R_{kk}/2$ and standardized anisotropy tensor $r_{ij} = (R_{ij} - 2k\delta_{ij}/3)/(2k)$. These equations read

$$\frac{\bar{\mathrm{D}}k}{\bar{\mathrm{D}}t} + \frac{1}{2\langle\rho\rangle}\frac{\partial\langle\rho\rangle T^R_{knn}}{\partial x_k} + 2k\left(r_{kn} + \frac{1}{3}\delta_{kn}\right)\frac{\partial\bar{U}_n}{\partial x_k} - 2k\, r_{kn}G^d_{nk} = -\frac{2\left(1 - c_0^{(\mathrm{PDF})}\right)k}{\tau_L^{(\mathrm{PDF})}}. \tag{3.7a}$$

$$\frac{\bar{\mathrm{D}}r_{ij}}{\bar{\mathrm{D}}t} + \frac{1}{2\langle\rho\rangle k}\frac{\partial\langle\rho\rangle(T^R_{kij} - T^R_{knn}\delta_{ij}/3)}{\partial x_k} + \frac{r_{ij}}{k}\frac{\bar{\mathrm{D}}k}{\bar{\mathrm{D}}t} + r_{ik}\left(\frac{\partial\bar{U}_j}{\partial x_k} - G^d_{jk}\right) + r_{jk}\left(\frac{\partial\bar{U}_i}{\partial x_k} - G^d_{ik}\right)$$
$$-\frac{2}{3}r_{kn}\left(\frac{\partial\bar{U}_n}{\partial x_k} - G^d_{nk}\right)\delta_{ij} = -\frac{2}{\tau_L^{(\mathrm{PDF})}}r_{ij} - \frac{1}{3}\left(2\bar{S}^d_{ij} - G^d_{ij} - G^d_{ji}\right), \tag{3.7b}$$

where $G^d_{ij} = G_{ij} - G_{nn}\delta_{ij}/3$ is the deviatoric component of G_{ij}. The comparison with the corresponding molecular equations reveals that these equations account for two processes in addition to the processes involved in (2.12a,b): dissipation of turbulent kinetic energy [the last term of (3.7a), which is equal to the negative dissipation rate ϵ] and turbulent kinetic energy redistribution (terms that contain G^d_{ij}). By comparing the Reynolds stress transport equation (3.6c) with the exact Reynolds stress transport equation which follows from averaging the Navier–Stokes equations [4, 11–12], one observes that terms related to compressibility effects and viscous and pressure transport terms do not appear explicitly in Eq. (3.6c). The effects of these terms are found to be small for many flows, but such contributions can be involved via the choice of G_{ij} in Eq. (3.6c). Compressibility effects, for example, can be taken into account by the specification of $\tau_L^{(\mathrm{PDF})}$ and G^d_{ij} [55].

3.4 Relaxation frequency models

A significant problem related to the application of the stochastic PDF model is given by the need to specify the deviatoric frequency G^d_{ij} in order to close Eqs. (3.2a,b). The most convenient way to address this problem is to use the r_{ij} transport equation (3.7b) for the calculation of G^d_{ij} in order to assure the correct treatment of the anisotropy of Reynolds stresses. However, Eq. (3.7b) only provides conditions for the symmetric component of G^d_{ij}. To determine G^d_{ij} completely one may assume that G^d_{ij} is a symmetric matrix, like the Reynolds stress tensor. The resulting extended Langevin model is completely defined in terms of the Reynolds stress tensor [12, 54, 55]. However, the use of such an implicit equation for G^d_{ij} is cumbersome to implement in complex flows: numerical stiffness problems can result from the need for successive matrix inversions. To calculate G^d_{ij} explicitly, one can apply the same approach as used for the molecular stress calculation in Sect. 2. By adopting $G^d_{ij} = G^d_{ji}$, the first order of approximation for G^d_{ij} is given by a zero right-hand side of (3.7b),

$$G^{d\,(1)}_{ij} = \frac{3}{\tau_L^{(\mathrm{PDF})}}r_{ij} + \bar{S}^d_{ij}. \tag{3.8}$$

By neglecting the deviatoric contribution due to triple correlations and using the first-order approximation $G^{d(1)}_{ij}$ on the left-hand side, G^d_{ij} is given in the second order of approximation by

$$G^{d\,(2)}_{ij} = \frac{3r_{ij}}{\tau_L^{(\mathrm{PDF})}} + \bar{S}^d_{ij} - \frac{9}{\tau_L^{(\mathrm{PDF})}}\left[r_{ik}r_{kj} - \frac{r_{nk}r_{kn}}{3}\delta_{ij}\right]$$
$$-\frac{3}{2}\left[r_{ik}\bar{\Omega}_{kj} + r_{jk}\bar{\Omega}_{ki}\right] + \frac{3r_{ij}}{2}\left(\frac{1}{k}\frac{\bar{\mathrm{D}}k}{\bar{\mathrm{D}}t} + \frac{2}{3}\bar{S}_{nn}\right) + \frac{3}{2}\frac{\bar{\mathrm{D}}r_{ij}}{\bar{\mathrm{D}}t}, \tag{3.9}$$

where $\bar{\Omega}_{ij}$ denotes the averaged rate-of-rotation tensor $\Omega_{ij} = (\partial U_i/\partial x_j - \partial U_j/\partial x_i)/2$. This model may be rewritten such that it has the same structure as the Haworth–Pope model [4, 48, 56, 57],

$$G_{ij}^{d\,(2)} = \frac{3}{2}\frac{\bar{\mathrm{D}}r_{ij}}{\bar{\mathrm{D}}t} + \left[\frac{3r_{nk}r_{kn}}{\tau_L^{(\mathrm{PDF})}} - \frac{1}{3}\bar{S}_{nn}\right]\delta_{ij} + \left[\frac{3}{\tau_L^{(\mathrm{PDF})}} + \frac{3}{2}\left(\frac{1}{k}\frac{\bar{\mathrm{D}}k}{\bar{\mathrm{D}}t} + \frac{2}{3}\bar{S}_{nn}\right)\right]r_{ij} - \frac{9}{\tau_L^{(\mathrm{PDF})}}r_{ik}r_{kj} + H_{ijkn}\frac{\partial \bar{U}_k}{\partial x_n}. \tag{3.10}$$

According to expression (3.9), the tensor H_{ijkn} is given by

$$H_{ijkn} = \frac{1}{2}\big[\delta_{ik}\delta_{jn} + \delta_{jk}\delta_{in}\big] - \frac{3}{2}\big[r_{ik}\delta_{jn} + r_{jk}\delta_{in} - r_{in}\delta_{jk} - r_{jn}\delta_{ik}\big]. \tag{3.11}$$

Compared to the Haworth–Pope model one observes that the model (3.10) does not require the calculation of 11 adjustable parameters for each flow considered. One also observes that (3.10) involves one additional term (the first term on the right-hand side).

Instead of assuming $G_{ij}^d = G_{ji}^{\mathrm{d}}$, the deviatoric component G_{ij}^d is often neglected in PDF models, which corresponds to the use of the simplified Langevin model $G_{ij} = -\delta_{ij}/\tau_L^{(\mathrm{PDF})}$. The latter assumption represents an approximation that is not always well satisfied. For incompressible flow, Sarkar's turbulent shear flow DNS [58] reveal for example $(G_{11}, G_{22}, G_{33}) = -(0.39, 0.52, 0.37)|\bar{S}|$. The equilibrium turbulent boundary layer DNS data of Moser et al. [59] demonstrate for a friction Reynolds number $Re_\tau = 590$ that $(G_{11}, G_{22}, G_{33}) = -(0.51, 0.76, 0.49)|\bar{S}|$. Here, $|\bar{S}| = (2\bar{S}_{kl}^d\bar{S}_{lk}^d)^{1/2}$ refers to the characteristic strain rate. With regard to these findings, the approximation $G_{ij}^d = 0$ is, therefore, related to deviations of 10–22%. With regard to compressible flows, such deviations may be larger provided the gradient Mach number becomes larger than unity [55, 58]. However, it is worth noting that such differences to DNS data do not have to imply corresponding shortcomings of simulations. Instead, the simplified Langevin model was applied successfully in many simulations (see, for example [60, 61] and the references therein).

In order to calculate the Reynolds stresses according to Eq. (3.7b) one has to define the deviatoric component G_{ij}^d. The extended Langevin model explains G_{ij}^d in terms of r_{ij} (it provides a mapping between G_{ij}^d and r_{ij}) such that this model cannot be used to calculate the Reynolds stresses. The simplified Langevin model, however, enables the Reynolds stress calculation due to the assumption $G_{ij}^d = 0$. In correspondence to the calculation of the molecular stress tensor in Sect. 2, the Reynolds stress tensor is given in the first order of approximation by

$$R_{ij}^{(1)} = \frac{2}{3}k\delta_{ij} - 2\nu^{(\mathrm{PDF})}\,\bar{S}_{ij}^d. \tag{3.12}$$

Here, the turbulent viscosity $\nu^{(\mathrm{PDF})} = k\tau_L^{(\mathrm{PDF})}/3$ is introduced. The latter expression recovers the standard model for $\nu^{(\mathrm{PDF})}$, which is given by

$$\nu^{(\mathrm{PDF})} = C_\mu\frac{k^2}{\varepsilon}, \tag{3.13}$$

where $C_\mu = 2(1-c_0^{(\mathrm{PDF})})/3$. By adopting $c_0^{(\mathrm{PDF})} = 5/6$ (see Sect. 5) one finds $C_\mu = 1/9$. This C_μ value agrees with the results of many investigations [4, 62]. Compressible channel-flow DNS data for different Reynolds and Mach numbers indicate $C_\mu = 0.11 \pm 0.03$ away from solid walls [63]. The second-order approximation of the Reynolds stress tensor R_{ij} is then given by

$$R_{ij}^{(2)} = \frac{2}{3}k\delta_{ij} - 2\nu^{(\mathrm{PDF})}\left(\bar{S}_{ij}^d - \frac{1}{2}\frac{\bar{\mathrm{D}}\tau_L^{(\mathrm{PDF})}\bar{S}_{ij}^d}{\bar{\mathrm{D}}t}\right) + \frac{3\big[\nu^{(\mathrm{PDF})}\big]^2}{k}\left[2\bar{S}_{ik}^d\bar{S}_{kj}^d - \frac{2}{3}\bar{S}_{nk}^d\bar{S}_{kn}^d\,\delta_{ij} - \bar{S}_{ik}^d\bar{\Omega}_{kj} - \bar{S}_{jk}^d\bar{\Omega}_{ki}\right]. \tag{3.14}$$

The model (3.14) represents the rescaled nonlinear molecular stress model (2.15). It extends the nonlinear model of Gatski and Speziale [64] by involving the derivative of $\tau_L^{(\mathrm{PDF})}\,\bar{S}_{ij}^d$, and it provides the parameters

β_1 and β_2 applied in Gatski and Speziale's model: $2\,\beta_1 = \beta_2 = 6\,C_\mu^2$. A specific feature of Eq. (3.14) is given by the fact that there is no contribution due to $\bar{\Omega}_{ik}\bar{\Omega}_{kj} - \bar{\Omega}_{nk}\bar{\Omega}_{kn}\delta_{ij}/3$, which appears in the models of Yoshizawa [65] and Rubinstein and Barton [66]. Speziale [67] showed that such a quadratic rate-of-rotation tensor contribution yields erroneous predictions for isotropic turbulence subjected to a solid-body rotation.

4 Small-scale turbulence modeling

The need to model all the spectrum of turbulent motions in PDF/RANS methods represents a nontrivial problem. For example, a universal model for the characteristic length scale L of large-scale turbulent eddies is unavailable, and complex methods are required to account accurately for the anisotropy of Reynolds stresses. A natural approach to overcome these problems is given by the replacement of ensemble averages by spatially filtered variables such that only small-scale processes have to be modeled. The essential features of such FDF/LES methods will be described next. Their characteristic advantages and disadvantages will be discussed in comparison to PDF/RANS methods in Sect. 5.1.

4.1 Filtered variables

FDF/LES methods calculate the dynamics of fluid dynamic variables that are filtered in space. In analogy to (2.1), we define mass-density-weighted filtered variables by

$$\tilde{Q}(\mathbf{x},t) = \frac{\langle \rho(\mathbf{x},t)\, Q\rangle_G}{\langle \rho(\mathbf{x},t)\rangle_G}, \tag{4.1}$$

where $\langle\cdots\rangle_G$ refers to a filtering in space that is defined by

$$\langle \rho(\mathbf{x},t) Q(\mathbf{x},t)\rangle_G = \int \mathrm{d}\mathbf{r}\;\; \rho(\mathbf{x}+\mathbf{r},\mathrm{t})\;\; \mathrm{Q}(\mathbf{x}+\mathbf{r},\mathrm{t})\;\; \mathrm{G}(\mathbf{r}). \tag{4.2}$$

The filter function G is assumed to be homogeneous, i.e., independent of $\mathbf{x}$. We assume $\int \mathrm{d}\mathbf{r}\, G(\mathbf{r}) = 1$ and $G(\mathbf{r}) = G(-\mathbf{r})$. Moreover, only positive filter functions are considered for which all the moments $\int \mathrm{d}\mathbf{r}\, \mathrm{r}^{\mathrm{m}} G(\mathbf{r})$ exist for $m \geq 0$ [19]. G has, therefore, the properties of a PDF.

The scale of filtering is defined by the filter width Δ, which is chosen such that $\Delta << L$. FDF or LES calculations are performed if $\eta << \Delta << L$, where η is the Kolmogorov length scale. We assume that G becomes a delta function (this means $G(\mathbf{r}) \to \delta(\mathbf{r})$) for $\Delta << \eta$. Relation (4.2) reveals that the effect of filtering then disappears. It will be shown in Sect. 4.4 that DNS is performed in the latter case.

4.2 Stochastic equations

In correspondence to the PDF model (3.2a,b), let us consider the following stochastic FDF velocity model which has been validated for several applications [21, 22, 27]:

$$\frac{\mathrm{d}}{\mathrm{d}t} x_i^* = U_i^*, \tag{4.3a}$$

$$\frac{\mathrm{d}}{\mathrm{d}t} U_i^* = \frac{2}{\langle\rho\rangle_G}\frac{\partial \langle\rho\rangle_G \tilde{\nu}\, \tilde{S}_{ik}^d}{\partial x_k} - \frac{1}{\langle\rho\rangle_G}\frac{\partial \langle p\rangle_G}{\partial x_i} - \frac{1}{\tau_L^{(\mathrm{FDF})}}\left(U_i^* - \tilde{U}_i\right) + \sqrt{\frac{4c_0^{(\mathrm{FDF})} k}{3\tau_L^{(\mathrm{FDF})}}}\frac{\mathrm{d}W_\mathrm{i}}{\mathrm{d}t}. \tag{4.3b}$$

Here, x_i^* and U_i^* represent the ith components of a fluid particle position and velocity. The transport terms (the first two terms on the right-hand side of (4.3b)) correspond to the transport terms in (3.2b): $\langle\rho\rangle_G$, $\langle \mathrm{p}\rangle_G$, $\tilde{\nu}$ and $\tilde{S}_{ik}^d$ denote the filtered fluid mass density, pressure, viscosity and deviatoric rate-of-strain tensor (ν and S_{ij}^d are again assumed to be uncorrelated), respectively. The relaxation term describes a relaxation towards the filtered velocity $\tilde{U}_i$ with a characteristic FDF relaxation time scale $\tau_L^{(\mathrm{FDF})}$. An anisotropic matrix G_{ij}^d is not involved. The latter assumption seems to represent an appropriate concept for the modeling of small-scale processes, in particular if a small filter width is used such that modeling assumptions applied to small-scale motions have

little influence on the dynamics of filtered variables (see Sect. 4.4). Nevertheless, this question cannot be seen to be completely clarified until now [68, 69]. k represents the residual turbulent kinetic energy (the same notation k is used as in the PDF model (3.2a,b) because k does not need modeling). The residual turbulent kinetic energy is defined by $k = D_{kk}/2$, where D_{ij} represents the subgrid-scale (SGS) stress tensor (the variance of the FDF, which is defined in correspondence to R_{ij}). The noise strength is controlled by the nondimensional parameter $c_0^{(\mathrm{FDF})}$. In analogy to relation (3.5), one finds $c_0^{(\mathrm{FDF})} = C_0^{(\mathrm{FDF})}/[C_0^{(\mathrm{FDF})} + 2/3]$. With regard to the FDF model (4.3a,b), $C_0^{(\mathrm{FDF})}$ agrees with the Kolmogorov constant C_K that determines the energy spectrum [23]. An analysis of implications of (4.3a,b) reveals that $C_0^{(\mathrm{FDF})} = 19/12 \approx 1.58$, which agrees very well with the conclusion $C_\mathrm{K} = 1.62 \pm 0.17$ of many measurements [70]. Thus, one finds $c_0^{(\mathrm{FDF})} = 19/27 \approx 0.7$ [23]. DNS results [21] support this finding very well, and investigations of the effects of $c_0^{(\mathrm{FDF})}$ variations on simulation results [21, 22] also confirm the suitability of $c_0^{(\mathrm{FDF})} \approx 0.7$.

The FDF model (4.3a,b) is unclosed as long as the relaxation time scale $\tau_L^{(\mathrm{FDF})}$ is not defined. According to Prandtl's mixing-length assumption [71], we write

$$\tau_L^{(\mathrm{FDF})} = \ell^{(\mathrm{FDF})}\, k^{-1/2}, \tag{4.4}$$

where $\ell^{(\mathrm{FDF})}$ refers to the characteristic length scale of SGS fluctuations. In contrast to the scaling of L involved in (3.4) for $\tau_L^{(\mathrm{PDF})}$, the significant advantage of the applied filtering in space is the fact that the scaling of the length scale $\ell^{(\mathrm{FDF})}$ is known. The length scale of SGS fluctuations has to be controlled by the filter width Δ, which justifies the assumption that $\ell^{(\mathrm{FDF})}$ is proportional to Δ . An analysis of this scaling reveals that $\ell^{(\mathrm{FDF})} = \ell_* \Delta$, where $\ell_* = (1 \pm 0.5)/3$ [23]. The latter implies

$$\tau_L^{(\mathrm{FDF})} = \ell_* \Delta\, k^{-1/2}\,. \tag{4.5}$$

By adopting available DNS data and studies of the effects of parameter variations on simulation results [21, 22], one can show that relation (4.5) is very well supported [23].

4.3 Deterministic equations

The consequences of the stochastic FDF model (4.3a,b) for the transport of filtered variables can be obtained in the same way as explained above with regard to molecular motion. By rewriting (4.3a,b) as the corresponding Fokker–Planck equation for the FDF, one obtains the following LES equations for the filtered mass density $\langle\rho\rangle_G$, velocity $\tilde{U}_i$, and SGS tensor D_{ij}:

$$\frac{\tilde{\mathrm{D}}\langle\rho\rangle_G}{\tilde{\mathrm{D}}t} = -\langle\rho\rangle_G \frac{\partial \tilde{U}_k}{\partial x_k}, \tag{4.6a}$$

$$\frac{\tilde{\mathrm{D}}\,\tilde{U}_i}{\tilde{\mathrm{D}}t} + \frac{1}{\langle\rho\rangle_G}\frac{\partial \langle\rho\rangle_G D_{ik}}{\partial x_k} = \frac{2}{\langle\rho\rangle_G}\frac{\partial \langle\rho\rangle_G \tilde{\nu}\,\tilde{S}_{ik}^d}{\partial x_k} - \frac{1}{\langle\rho\rangle_G}\frac{\partial \langle p\rangle_G}{\partial x_i}, \tag{4.6b}$$

$$\frac{\tilde{\mathrm{D}}D_{ij}}{\tilde{\mathrm{D}}t} + \frac{1}{\langle\rho\rangle_G}\frac{\partial \langle\rho\rangle_G T_{kij}^D}{\partial x_k} + D_{ik}\frac{\partial \tilde{U}_j}{\partial x_k} + D_{jk}\frac{\partial \tilde{U}_i}{\partial x_k} = -\frac{2}{\tau_L^{(FDF)}}\left(D_{ij} - \frac{2}{3}c_0^{(\mathrm{FDF})} k \delta_{ij}\right). \tag{4.6c}$$

Here, $\tilde{\mathrm{D}}/\tilde{\mathrm{D}}t = \partial/\partial t + \tilde{U}_k\, \partial/\partial x_k$ denotes the filtered Lagrangian time derivative, and T_{kij}^D is the triple correlation tensor of the SGS velocity fluctuations (corresponding to T_{kij}^R in Eq. (3.6c)).

In correspondence to the molecular equations (2.12a,b), Eq. (4.6c) for the SGS stress tensor $D_{ij} = 2k(\delta_{ij}/3 + d_{ij})$ can be rewritten in terms of equations for the residual turbulent kinetic energy $k = D_{kk}/2$ and

the standardized anisotropy tensor $d_{ij} = (D_{ij} - 2k\delta_{ij}/3)/(2k)$. These equations read

$$\frac{\tilde{\mathrm{D}}k}{\tilde{\mathrm{D}}t} + \frac{1}{2\langle\rho\rangle_G}\frac{\partial\langle\rho\rangle_G T^D_{knn}}{\partial x_k} + 2k\left(d_{kn} + \frac{1}{3}\delta_{kn}\right)\frac{\partial\tilde{U}_n}{\partial x_k} = -\frac{2\left(1 - c_0^{(\mathrm{FDF})}\right)k}{\tau_L^{(\mathrm{FDF})}}. \tag{4.7a}$$

$$\begin{aligned}\frac{\tilde{\mathrm{D}}d_{ij}}{\tilde{\mathrm{D}}t} + \frac{1}{2\langle\rho\rangle_G k}\frac{\partial\langle\rho\rangle_G(T^D_{kij} - T^D_{knn}\delta_{ij}/3)}{\partial x_k} + \frac{d_{ij}}{k}\frac{\tilde{\mathrm{D}}k}{\tilde{\mathrm{D}}t} + d_{ik}\frac{\partial\tilde{U}_j}{\partial x_k} + d_{jk}\frac{\partial\tilde{U}_i}{\partial x_k} - \frac{2}{3}d_{kn}\frac{\partial\tilde{U}_n}{\partial x_k}\,\delta_{ij} \\ = -\frac{2}{\tau_L^{(\mathrm{FDF})}}d_{ij} - \frac{2}{3}\tilde{S}^d_{ij}.\end{aligned} \tag{4.7b}$$

The first-order approximation for the anisotropy tensor d_{ij} is then given by the balance of the terms on the right-hand side of (4.7b): $d^{(1)}_{ij} = -\tilde{S}^d_{ij}\tau_L^{(\mathrm{FDF})}/3$. The latter result implies the following expression for the SGS stress tensor D_{ij} in the first order of approximation,

$$D^{(1)}_{ij} = \frac{2}{3}k\delta_{ij} - 2\nu^{(\mathrm{FDF})}\,\tilde{S}^d_{ij}, \tag{4.8}$$

where the SGS viscosity $\nu^{(\mathrm{FDF})} = k\tau_L^{(\mathrm{FDF})}/3$ is introduced. By adopting expression (4.5) for $\tau_L^{(\mathrm{FDF})}$, the SGS viscosity $\nu^{(\mathrm{FDF})}$ is given by

$$\nu^{(\mathrm{FDF})} = \Delta\, k^{1/2}/9. \tag{4.9}$$

This parametrization for $\nu^{(\mathrm{FDF})}$ has been used in several applications [4, 72, 73]. To recover the Smagorinsky model we assume a balance between the production and dissipation in (4.7a) given by $d^{(1)}_{kn}\partial\tilde{U}_n/\partial x_k\tau_L^{(\mathrm{FDF})} = c_0^{(\mathrm{FDF})} - 1$. By introducing the characteristic strain rate $|\tilde{S}| = (2\tilde{S}^d_{kl}\tilde{S}^d_{lk})^{1/2}$ and adopting $d^{(1)}_{ij} = -\tilde{S}^d_{ij}\tau_L^{(\mathrm{FDF})}/3$ and $c_0^{(\mathrm{FDF})} = 19/27$, one finds $|\tilde{S}|\ \tau_L^{(\mathrm{FDF})} = 4/3$. Combined with $\tau_L^{(\mathrm{FDF})} = \Delta k^{-1/2}/3$ according to relation (4.5), the latter expression provides $k^{1/2} = \Delta|\tilde{S}|\ /4$. Hence, expression (4.9) can be written

$$\nu^{(\mathrm{FDF})} = c_S\Delta^2|\tilde{S}|, \tag{4.10}$$

where the Smagorinsky coefficient is given by $c_{\mathrm{S}} = (1/6)^2$. This latter value for the Smagorinsky coefficient c_{S} corresponds to the standard value for this parameter [4, 72]. The coefficient c_{S} can also be calculated by a dynamic procedure [74, 75]. The latter approach avoids the problem of finding an appropriate constant c_{S} value, and it enables the use of different c_{S} values for various flow regions.

In the second-order approximation, the SGS stress D_{ij} is given in correspondence to (2.15) by

$$\begin{aligned}D^{(2)}_{ij} = \frac{2}{3}k\delta_{ij} - 2\nu^{(\mathrm{FDF})}\left(\tilde{S}^d_{ij} - \frac{1}{2}\frac{\tilde{\mathrm{D}}\tau_L^{(\mathrm{FDF})}\tilde{S}^d_{ij}}{\tilde{\mathrm{D}}t}\right) \\ + \frac{3\left[\nu^{(\mathrm{FDF})}\right]^2}{k}\left[2\tilde{S}^d_{ik}\tilde{S}^d_{kj} - \frac{2}{3}\tilde{S}^d_{nk}\tilde{S}^d_{kn}\,\delta_{ij} - \tilde{S}^d_{ik}\tilde{\Omega}_{kj} - \tilde{S}^d_{jk}\tilde{\Omega}_{ki}\right].\end{aligned} \tag{4.11}$$

$\tilde{\Omega}_{ij}$ refers to the filtered rate-of-rotation tensor. In contrast to the low relevance of nonlinear terms in (2.15) with regard to small-Knudsen-number flows, one finds that nonlinear terms in (4.11) may well be relevant [23]. The advantage of deriving nonlinear contributions as a consequence of a stochastic model is given by the fact that one obtains consistent expressions for all model coefficients (which is otherwise a nontrivial problem [76–78]). It is worth noting that the coefficients of linear and nonlinear terms in (4.11) can also be calculated by a dynamic procedure [79, 80].

4.4 The DNS limit

To prepare for the discussion in Sect. 5, let us have a closer look at the limit case that the filter width $\Delta << \eta$, where η refers to the Kolmogorov length scale. To do this, it is helpful to consider first the equations for SGS velocity fluctuations that are implied by the stochastic model (4.3a,b) and the filtered equations (4.6a,b). These equations for velocity fluctuations read

$$\frac{\mathrm{d}}{\mathrm{d}t}x_i^* = U_i^*, \tag{4.12a}$$

$$\frac{\mathrm{d}}{\mathrm{d}t}\left(U_i^* - \tilde{U}_i\right) = -\left[\frac{\delta_{ik}}{\tau_L^{(\mathrm{FDF})}} + \frac{\partial \tilde{U}_i}{\partial x_k}\right]\left(U_k^* - \tilde{U}_k\right) + \frac{1}{\langle\rho\rangle_G}\frac{\partial \langle\rho\rangle_G D_{ik}}{\partial x_k} + \sqrt{\frac{4c_0^{(\mathrm{FDF})}k}{3\tau_L^{(\mathrm{FDF})}}}\frac{\mathrm{d}W_\mathrm{i}}{\mathrm{d}t}. \tag{4.12b}$$

The results presented in Sect. 4.3 show that the residual turbulent kinetic energy $k = (\Delta|\tilde{S}|/4)^2$ and SGS viscosity $\nu^{(\mathrm{FDF})} = \Delta k^{1/2}/9$ disappear for $\Delta << \eta$. Correspondingly, the SGS stress tensor D_{ik} disappears, too. The last two terms in (4.12b) disappear, therefore, for $\Delta << \eta$ ($\tau_L^{(\mathrm{FDF})}$ remains finite because $|\tilde{S}|\,\tau_L^{(\mathrm{FDF})} = 4/3$; see above), which means that there is no stochastic forcing. In consistency with the vanishing residual turbulent kinetic energy k we set $U_k^* = \tilde{U}_k$ initially for the integration of (4.12b). Then, Eq. (4.12b) predicts zero velocity fluctuations for all times.

For the case of vanishing SGS fluctuations, filtered variables have to be equal to their instantaneous variables [which implies $G(\mathbf{r}) \to \delta(\mathbf{r})$ for $\Delta << \eta$ as assumed in Sect. 4.1]. By neglecting all effects of filtering in (4.6a,b), the equations for filtered variables reduce to

$$\frac{\mathrm{D}\rho}{\mathrm{D}t} = -\rho\frac{\partial U_k}{\partial x_k}, \tag{4.13a}$$

$$\frac{\mathrm{D}\,U_i}{\mathrm{D}t} = \frac{2}{\rho}\frac{\partial \rho\nu\, S_{ik}^d}{\partial x_k} - \frac{1}{\rho}\frac{\partial p}{\partial x_i}. \tag{4.13b}$$

$\mathrm{D}/\mathrm{D}t = \partial/\partial t + U_\mathrm{k}\partial/\partial x_k$ is the Lagrangian time derivative as applied above. Equations (4.13a,b) recover (2.11a,b) combined with Eq. (2.13) for the molecular stress tensor, where the pressure p is given by $2\rho e/3$. Hence, the model (4.3a,b) recovers DNS equations for $\Delta << \eta$. The influence of SGS fluctuation models on the dynamics of filtered variables becomes, therefore, smaller with decreasing filter width, which provides support for the use of relatively simple fluctuation models (without anisotropic relaxation).

5 Unified turbulence models

After considering PDF/RANS and FDF/LES methods in Sects. 3 and 4, respectively, let us have a closer look at the characteristic advantages and disadvantages of these methods and their consequences.

5.1 The need to develop unified turbulence models

The application of the stochastic PDF model (3.2a,b) to flow simulations is much more efficient than the use of DNS, but this approach also faces significant problems. A first question is related to the deviatoric matrix G_{ik}^d, which has to be provided to describe the turbulent energy redistribution correctly. This problem can be solved as described in Sect. 3, but the required calculation of Reynolds stresses represents a significant source of numerical error due to the finite number of realizations used in simulations. A second question is related to the isotropic noise source applied in (3.2b). In correspondence to the modeling of the relaxation of velocity fluctuations, one may expect in general a noise-term structure given by $b_{ik}\mathrm{d}W_k/\mathrm{dt}$, where b_{ik} is any anisotropic matrix. Indeed, there seem to be indications that such an anisotropic matrix b_{ik} should be considered, in particular with regard to flows with relatively low Reynolds number [81]. However, the question of how such a matrix b_{ik} should be modeled remains unsolved until now. A third question is related to the need to provide the characteristic length scale L of large-scale turbulent eddies in relation (3.4) for $\tau_L^{(\mathrm{PDF})}$. The generality of concepts applied currently to provide a corresponding scale-determining equation is certainly questionable [63].

The relevance of such modeling issues seems to be much lower when adopting FDF/LES methods, but the use of these methods may require infeasible computational costs. FDF simulations are six times less expensive than DNS, but they may require 15–30 times more effort than LES methods [21]. Similarly, the use of LES will be too expensive for many applications. In regions away from solid walls the number of grid points required for LES scales with the Reynolds number Re according to $Re^{0.4}$, but the resolution of near-wall motions requires a number of grid points that increases proportional to $Re^{1.76}$ [82]. The required number of grid points is then nearly the same as for DNS, which is characterized by a $Re^{9/4}$ scaling [83, 84]; see the illustration in Fig. 1. Consequently, such simulations become infeasible for high-Reynolds-number flows such as those that occur in aeronautical and meteorological applications. In contrast, the RANS grid requires clustering only in the wall-normal direction so that the grid requirements are proportional to $\ln(Re)$ [4, 30], and the RANS grid requirements away from solid walls are independent of Re.

Due to the demanding computational requirements related to FDF/LES methods, at least the simulation of high-Reynolds number wall-bounded flows requires, therefore, combinations of FDF and PDF, or LES and RANS methods. The use of consistent combinations appears to be helpful to perform accurate computations. Thus, there is a need for the development of unified turbulence models that may be used depending on the resolution as FDF or PDF, LES or RANS methods. From a more general point of view, the development of such methods appears to be helpful for the improvement of the efficiency and accuracy of turbulence simulations (see the illustration in Fig. 2): accurate FDF and LES calculations could be applied to assess and improve the performance of more-efficient PDF and RANS calculations. Also from a theoretical point of view, the development of unified turbulence models is relevant: a common modeling strategy may well contribute to model developments.

However, the construction of such unified models turned out to be a nontrivial problem. Previously presented suggestions addressed this problem by considering the question of how it is possible to find a generalized stress tensor that recovers the Reynolds stress and SGS stress tensors in limits [12, 17, 28–31]. The stress tensor is the result of a variety of physical processes. It is, therefore, impossible to find support for the construction of a generalized stress tensor by taking reference to a simple physical explanation of scale effects. The only way to develop generalized stress tensor models is then given by the application of heuristic interpolation procedures between RANS and LES limits. Many different suggestions were presented for that, and the assessment of differences between such suggestions turned out to be a complicated problem. A general formal solution to this question considered was presented recently by Germano in conjunction with an analysis of all the problems related to the application of this approach [31].

5.2 The unification of stochastic velocity models

As an alternative to existing approaches, the question of how it is possible to construct unified models for compressible turbulent flows will be addressed here at the level of stochastic turbulence models. This approach is very helpful because it implies a separate consideration of the evolution of velocity fluctuations and their characteristic time scales. The discussions in Sects. 3 [see (3.2a,b)] and 4 [see (4.3a,b)] show that the generalized Langevin model represents an appropriate basis for the modeling of velocities fields,

$$\frac{\mathrm{d}}{\mathrm{d}t}x_i^* = U_i^*, \tag{5.1a}$$

$$\frac{\mathrm{d}}{\mathrm{d}t}U_i^* = \frac{2}{\langle\rho\rangle_G}\frac{\partial\langle\rho\rangle_G\tilde{\nu}\,\tilde{S}_{ik}^d}{\partial x_k} - \frac{1}{\langle\rho\rangle_G}\frac{\partial\langle p\rangle_G}{\partial x_i} - \frac{1}{\tau_L}\Big[\delta_{ik} - \tau_L G_{ik}^d\Big]\Big(U_k^* - \tilde{U}_k\Big) + \sqrt{\frac{4c_0k}{3\tau_L}}\frac{\mathrm{d}W_i}{\mathrm{d}t}. \tag{5.1b}$$

Here, τ_L and c_0 are used without superscripts (which were applied above to indicate the FDF and PDF limits of τ_L and c_0). G_{ik}^d is assumed to be given as explained in Sect. 3.

The filtered variables involved in (5.1a,b) are defined as spatially filtered variables according to (4.1). The properties of the stochastic model (5.1a,b) depend essentially on the choice of the filter function G that is controlled, basically, by the filter width Δ. In particular, the properties of (5.1a,b) are determined by the ratio of Δ to several characteristic length scales. A first case (the small-Δ limit) is given by adopting a small filter width $\Delta << L$, where L is the characteristic length scale of large-scale motions. FDF/LES calculations are then performed by adopting $\eta << \Delta << L$ (η is the Kolmogorov length scale), and DNS is performed by adopting $\Delta << \eta$ (see Sect. 4.4). A second case (the large-Δ limit) is given by choosing Δ very large, $L << \Delta << L_0$, where L_0 characterizes the length scale of the largest eddies that are injected into the flow.

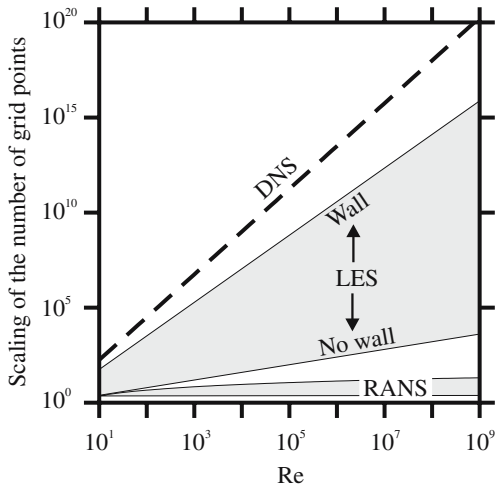

Fig. 1 An illustration of the scaling of the number of grid points with the Reynolds number Re for different methodologies. The use of DNS is characterized by a $Re^{9/4}$ scaling [83–84]. In regions away from a solid wall the number of grid points required for LES scales with $Re^{0.4}$, but the resolution of near-wall motions requires a number of grid points that increases proportional to $Re^{1.76}$ [82]. In contrast, the RANS grid requirements are proportional to ln(Re) [4, 30]. Away from a solid wall the RANS grid is independent of Re

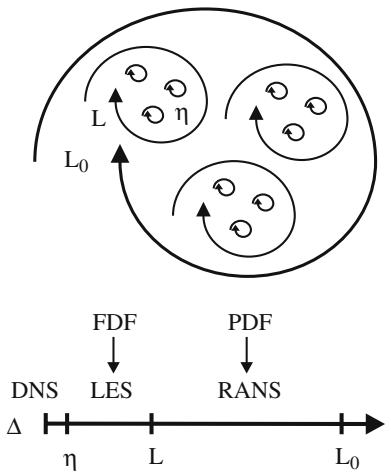

Fig. 2 An illustration of unified turbulence models. A sketch of the energy cascade is given by eddies of the order L_0 (eddies that are injected into the flow), L (large-scale eddies) and η (Kolmogorov-scale eddies). The method applied depends on the choice of the filter width Δ . One applies a RANS method if $L << \Delta << L_0$, a LES method if $\eta << \Delta << L$, and DNS if $\Delta << \eta$. The appearance of filtered chemical reaction rates in models for reacting flows can be avoided by generalizing the RANS and LES methods to the PDF and FDF methods, respectively

To prove the suitability of the stochastic model (5.1a,b) as a unified turbulence model, let us compare the small-Δ and large-Δ limits of (5.1a,b) with the FDF model (4.3a,b) and PDF model (3.2a,b).

Regarding the small-Δ limit of (5.1a,b) one observes only one difference to (4.3a,b): the FDF model (4.3a,b) is generalized by involving the deviatoric frequency G_{ij}^d according to (3.2a,b). This consideration of G_{ij}^d is an option that assures a common structure of FDF and PDF models, but this approach may be related to some disadvantages; see Sect. 5.1. Another option is given by the neglect of G_{ij}^d in (5.1a,b). The suitability of the resulting FDF model was proved in a variety of investigations and applications (see Sect. 4), and the resulting PDF model represents a reasonable model (see Sect. 3) as long as the gradient Mach number is smaller than unity [55].

Regarding the large-Δ limit of the stochastic model (5.1a,b) one observes that (5.1a,b) recovers the PDF model (3.2a,b) with one exception: spatially filtered variables are applied in (5.1a,b) whereas ensemble averages are used in the PDF model (3.2a,b). An ensemble average is defined as a mean over all possible values

of a variable considered at any position and time. The use of a sufficiently large filter width $\Delta >> L$ is then an obvious requirement to involve values of all the energy spectrum. Do such spatially averaged variables represent ensemble means? The latter is strictly only the case if turbulence statistics do not change in space, that is, for statistically homogeneous flows. With regard to inhomogeneous flows one calculates variables in this way which are both ensemble-averaged (in the sense that all possible values of a variable considered are involved) and smoothed in space; this means that one calculates variables that are somewhat coarser than strict ensemble means. The use of such smoothed ensemble means represents a valid concept provided the smoothing in space allows an appropriate characterization of spatial variations of the flow considered. It is worth noting that exactly this type of averaging is applied to solve PDF transport equations numerically (in stochastic particle methods one calculates ensemble averages as means over an ensemble of particles inside a box considered [4]). Thus, the large-Δ limit of (5.1a,b) represents a PDF model.

5.3 The unification of time-scale models

The stochastic model (5.1a,b) is unclosed as long as the time scale τ_L of turbulent motions is not defined. In particular, τ_L should recover $\tau_L^{(\mathrm{PDF})} = 2(1 - c_0^{(\mathrm{PDF})}) L\, k^{-1/2}$ according to the PDF limit (3.4) and $\tau_L^{(\mathrm{FDF})} = \ell_* \Delta \mathrm{k}^{-1/2}$ according to the FDF limit (4.5). First, we assume again

$$\tau_L = \ell\, k^{-1/2}. \tag{5.2}$$

The characteristic length scale ℓ of turbulent fluctuations will be defined by $\ell = \ell_* T_\lambda L$. Here, $L = k^{3/2}/\varepsilon$ is the characteristic length scale of large-scale eddies, and a transfer function T_λ is introduced (which may depend on any parameter λ; see below). By adopting $\ell_* = 1/3$ as above, we obtain

$$\tau_L = \ell_* T_\lambda\, L\, k^{-1/2}. \tag{5.3}$$

The PDF and FDF limits of τ_L provide support for the following PDF and FDF limits of T_λ,

$$T_\lambda = \begin{cases} \Delta/L & \text{if } \Delta/L << 1, \\ 1 & \text{if } \Delta/L >> 1. \end{cases} \tag{5.4}$$

According to (5.4), the FDF limit of τ_L is given by $\tau_L^{(\mathrm{FDF})} = \ell_* \Delta \mathrm{k}^{-1/2}$, which recovers (4.5). The PDF limit $\tau_L^{(\mathrm{PDF})} = \ell_*\, L\, k^{-1/2}$ recovers relation (3.4), where $\ell_* = 2(1 - c_0^{(\mathrm{PDF})})$. By adopting $\ell_* = 1/3$ we find $c_0^{(\mathrm{PDF})} = 5/6 \approx 0.83$, which agrees with the result $c_0^{(\mathrm{PDF})} = 0.83 \pm 0.07$ of many other investigations regarding the range of $c_0^{(\mathrm{PDF})}$ variations (see Sect. 3). To take c_0 variations in the FDF and PDF limits into account, one may generalize this parameter by $c_0 = 19/27 + 7T_\lambda/54$ (but the effect of such small c_0 variations will be very limited; see the discussion in Sect. 5.4).

To obtain a continuous model for T_λ it is convenient to consider instead of relation (5.4) the derivative $\mathrm{d}T_\lambda/\mathrm{d}(\Delta/L)$, because this quantity is bounded by zero and unity,

$$\frac{\mathrm{d}T_\lambda}{\mathrm{d}(\Delta/L)} = \begin{cases} 1 & \text{if } \Delta/L << 1, \\ 0 & \text{if } \Delta/L >> 1. \end{cases} \tag{5.5}$$

This relation shows that $1 - \mathrm{d}T_\lambda/\mathrm{d}(\Delta/L)$ may be considered as a distribution function which will be denoted by $\theta_\lambda(\Delta/L - 1)$; the probability for the large-Δ limit is equal to zero for $\Delta/L << 1$ and equal to one for $\Delta/L >> 1$. By adopting $\theta_\lambda(\Delta/L - 1) = 1 - \theta_\lambda(1 - \Delta/L)$, relation (5.5) can be rewritten as

$$\frac{\mathrm{d}T_\lambda}{\mathrm{d}(\Delta/L)} = \theta_\lambda(1 - \Delta/L). \tag{5.6}$$

The transfer function T_λ can then be obtained by integrating (5.6),

$$T_\lambda = \int_0^{\Delta/L} \mathrm{d}y\; \theta_\lambda(1 - y). \tag{5.7}$$

Thus, the transfer function T_λ depends on the specification of the distribution function $\theta_\lambda(1 - \Delta/L)$.

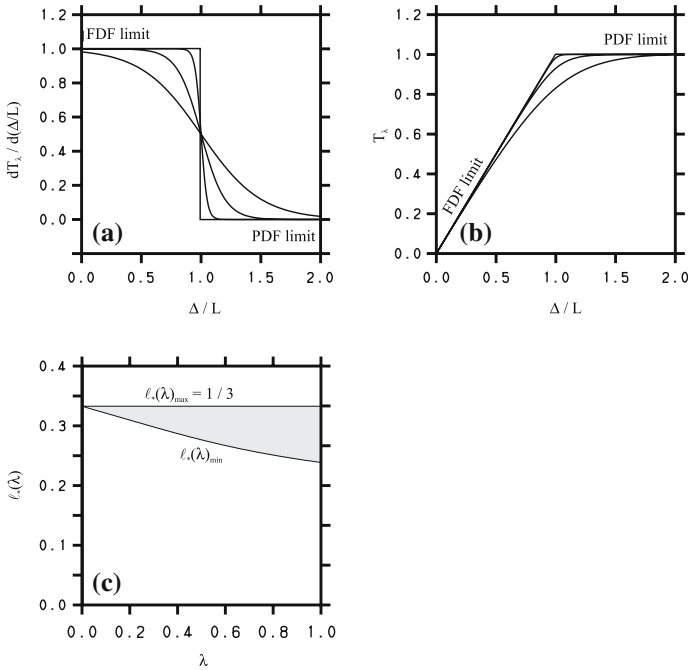

Fig. 3 The derivative $dT_\lambda/d(\Delta/L)$ and T_λ are shown in **a** and **b** according to (5.6)–(5.9) for values $\lambda = (0, 0.05, 0.2, 0.5)$; the functions decrease with growing λ for $\Delta/L \leq 1$. Δ is the filter width and $L = k^{3/2}/\epsilon$ is the characteristic length scale of large-scale eddies. For $\lambda \to 0$, these curves recover $dT/d(\Delta/L)$ and T, respectively. **c** The variation of $\ell_*(\lambda)$. The corresponding minimum and maximum values are given by (5.13)

5.4 The evaluation of the unified time-scale model

To address the relevance of different choices of the distribution function $\theta_\lambda(1 - \Delta/L)$ in Eq. (5.7), let us consider a smooth generalization of the theta function (which allows a smooth transition between zero and one depending on parameter variations $0 \leq \lambda \leq 1$),

$$\theta_\lambda\left(1 - \frac{\Delta}{L}\right) = \frac{1}{2} + \frac{1}{2}\tanh\left(\frac{1 - \Delta/L}{\lambda}\right). \tag{5.8}$$

According to (5.7), we obtain a continuous and smooth function T_λ,

$$T_\lambda = \frac{\Delta}{2L} - \frac{\lambda}{2}\ln\left(\frac{\cosh\left((1 - \Delta/L)/\lambda\right)}{\cosh(1/\lambda)}\right). \tag{5.9}$$

Examples for T_λ and $dT_\lambda/d(\Delta/L)$ are given in Fig. 3 for several values of λ. It is worth noting that the right-hand side of (5.9) recovers the theta function $\theta(1 - \Delta/L)$ for $\lambda \to 0$. The corresponding limit T of T_λ represents the extrapolation of the trends given by (5.4),

$$T = \lim_{\lambda\to 0} T_\lambda = \int_0^{\Delta/L} dy\, \theta(1 - y) = \begin{cases} \Delta/L & \text{if } \Delta/L \leq 1, \\ 1 & \text{if } \Delta/L \geq 1. \end{cases} \tag{5.10}$$

To assess the relevance of the transition parameter λ, let us rewrite τ_L as

$$\tau_L(\lambda) = \ell_* T_\lambda\, L\, k^{-1/2} = \ell_*(\lambda) T\, L\, k^{-1/2}, \tag{5.11}$$

where $\ell_*(\lambda) = \ell_* T_\lambda/T$ is introduced ($\ell_* = 1/3$ as above). A closer look at the variation of $\ell_*(\lambda)$ then reveals the following range of variations:

$$\ell_*(\lambda)_{\min} \leq \ell_*(\lambda) \leq \ell_*(\lambda)_{\max}. \tag{5.12}$$

Here, the minimum $\ell_*(\lambda)_{\min}$ at $\Delta/L = 1$ and maximum $\ell_*(\lambda)_{\max}$ of λ_* are given by

$$\ell_*(\lambda)_{\min} = \left(\frac{1}{2} + \frac{\lambda}{2}\ln\left(\cosh(1/\lambda)\right)\right)\ell_*, \quad \ell_*(\lambda)_{\max} = \ell_*. \tag{5.13}$$

The corresponding range of variations of $\ell_*(\lambda)$ is shown in Fig. 3c. With regard to the parameter values $\lambda = (0.05; 0.2; 0.5)$ applied in Fig. 3a,b, we see that $\ell_*(\lambda)_{\min} = (0.33; 0.31; 0.28)$. It is worth noting that the calculation of ℓ_* on the basis of DNS data shows ℓ_* variations that may well be larger than the range of variations obtained here [23]. Available experience related to studies of the relevance of parameter variations to FDF simulations [27] indicates that the relevance of such minor ℓ_* modifications will be very low.

As a result of this discussion, it appears to be well justified to consider T_λ to be independent of λ, which corresponds to the limit $\lambda \to 0$, where $T_\lambda \to T$. In this case, the model (5.3) combined with $T_\lambda = T$ provides a simple physical explanation for resolution effects (see the illustration in Fig. 2). For $\Delta \leq L$ we find $\ell = \ell_*\Delta$. This dependence of ℓ on Δ is plausible; Δ determines the correlation length of fluctuations as long as $\Delta \leq L$. For $\Delta \geq L$ we find $\ell = \ell_* L$. This result is also plausible because the correlation length of fluctuations cannot become larger than the large eddy length scale L. It is worth noting that the definition of L is unconstrained. This length scale can be provided by a variety of methods [4, 7] that may well involve several relevant length or time scales [53].

6 Summary

This study can be summarized in the following way. First, stochastic PDF and FDF and deterministic RANS and LES methods for the modeling of turbulent flows (which can be described by the compressible Navier–Stokes equations) were described and compared with equations for molecular motion. On this basis it was shown that there is a need for the development of unified turbulence models that can be used continuously to perform LES and RANS, FDF and PDF simulations. It was also shown that the question of how it is possible to develop unified models for compressible turbulent flows should be addressed on the basis of stochastic methods. Compared to previous studies of this question based on deterministic LES and RANS methods [12, 17, 28–31], the advantage of considering stochastic FDF and PDF methods is given by the fact that the development of unified turbulence models can be concentrated on the generalization of characteristic time scales of turbulent velocity fluctuations.

A main result obtained here is the generalized relation $\tau_L = \ell_* T L k^{-1/2}$ for the characteristic time scale of turbulent velocity fluctuations, which provides a simple physical explanation for scale effects. The suitability of the unified stochastic turbulence model (5.1a,b) combined with $\tau_L = \ell_* T L k^{-1/2}$ was demonstrated by showing its correct behavior in the FDF and PDF limits. Regarding the transition between these limits it was shown that available experience indicates that the use of more-complex models (which depend on the choice of λ in (5.9)) will hardly be relevant to applications. Deterministic LES and RANS models can be obtained as a consequence of the unified stochastic model (see Sects. 3,4). These models recover and extend the well-known linear and nonlinear LES and RANS models for the SGS and Reynolds stress tensors. Dynamic formulations of these stress models can also be used, which enables the use of different parameter values for various flow regions.

Acknowledgements I am thankful to the referees for their very helpful suggestions for improvements. I would also like to thank Professor D. Roekaerts for valuable comments.

References

1. Givi, P.: Model-free simulations of turbulent reactive flows. Prog. Energy Combust. Sci. **15**, 1–107 (1989)
2. Moin, P., Mahesh, K.: Direct numerical simulation: a tool for turbulence research. Annu. Rev. Fluid Mech. **30**, 539–578 (1998)
3. Pope, S.B.: A perspective on turbulence modeling. In: Salas, M.D., Hefner, J.N., Sakell, L. (eds.) Modeling Complex Turbulent Flows, pp. 53–67. Kluwer, Dordrecht (1999)
4. Pope, S.B.: Turbulent Flows. Cambridge University Press, Cambridge (2000)
5. Poinsot, T., Veynante, D.: Theoretical and Numerical Combustion, Second edition. Edwards, Philadelphia (2005)
6. Hanjalić, K.: Advanced turbulence closure models: a view of current status and future prospects. Int. J. Heat Fluid Flow **15**, 178–203 (1994)
7. Wilcox, D.C.: Turbulence Modeling for CFD, Second edition. DCW Industries, La Cañada (1998)

8. Durbin, P.A., Petterson, B.A.: Statistical Theory and Modeling for Turbulent Flows. Wiley, Chichester (2001)
9. Pope, S.B.: PDF methods for turbulent reactive flows. Prog. Energy Combust. Sci. **11**, 119–192 (1985)
10. Dopazo, C.: Recent developments in PDF methods. In: Libby, P.A., Williams, F.A. (eds.) Turbulent Reacting Flows (Chap. 7) pp. 375–474. Academic, London (1994)
11. Fox, R.O.: Computational Models for Turbulent Reacting Flows. In: Cambridge Series in Chemical Engineering, Cambridge University Press, Cambridge (2003)
12. Heinz, S.: Statistical Mechanics of Turbulent Flows. Springer, Berlin Heidelberg New York (2003)
13. Heinz, S.: On Fokker–Planck equations for turbulent reacting flows. Part 1: Probability density function for Reynolds-averaged Navier–Stokes equations. Flow Turb. Combust. **70**, 115–152 (2003)
14. Piomelli, U.: Large eddy simulation: achievements and challenges. Prog. Aerosp. Sci. **35**, 335–362 (1999)
15. Germano, M.: Fundamentals of large eddy simulation. In: Peyret, R., Krause, E. (eds.) Advanced Turbulent Flows Computations. CISM Courses and Lectures 395, pp. 81–130. Springer, Berlin Heidelberg New York (2000)
16. Menevau, C., Katz, J.: Scale-invariance and turbulence models for large eddy simulation. Annu. Rev. Fluid Mech. **32**, 1–32 (2000)
17. Sagaut, P.: Large Eddy Simulation for Incompressible Flows, Second edition. Springer, Berlin Heidelberg New York (2002)
18. Lesieur, M., Métais, O., Comte, P.: Large-Eddy Simulations of Turbulence. Cambridge University Press, Cambridge (2005)
19. Colucci, P.J., Jaberi, F.A., Givi, P., Pope, S.B.: Filtered density function for large eddy simulations of turbulent reactive flows. Phys. Fluids **10**, 499–515 (1998)
20. Jaberi, F.A., Colucci, P.J., James, S., Givi, P., Pope, S.B.: Filtered mass density function for large eddy simulation of turbulent reacting flows. J. Fluid Mech. **401**, 85–121 (1999)
21. Gicquel, L.Y.M., Givi, P., Jaberi, F.A., Pope, S.B.: Velocity filtered density function for large eddy simulation of turbulent flows. Phys. Fluids **14**, 1196–1213 (2002)
22. Sheikhi, M.R.H., Drozda, T.G., Givi, P., Pope, S.B.: Velocity-scalar filtered density function for large eddy simulation of turbulent flows. Phys. Fluids **15**, 2321–2337 (2003)
23. Heinz, S.: On Fokker–Planck equations for turbulent reacting flows. Part 2. Filter density function for large eddy simulation. Flow Turb. Combust. **70**, 153–181 (2003)
24. Sheikhi, M.R.H., Drozda, T.G., Givi, P., Jaberi, F.A., Pope, S.B.: Large eddy simulation of a turbulent nonpremixed piloted methane jet flame (Sandia Flame D). Proc. Combust. Inst. **30**, 549–556 (2005)
25. Raman, V., Pitsch, H., Fox, R.O.: Hybrid large eddy simulation/Lagrangian filtered-density-function approach for simulating turbulent combustion. Combust. Flame **143**, 56–78 (2005)
26. Pitsch, H.: Large eddy simulation of turbulent combustion. Annu. Rev. Fluid Mech. **38**, 453–482 (2006)
27. Givi, P.: Filtered density function for subgrid scale modeling of turbulent combustion. AIAA J. **44**, 16–23 (2006)
28. Speziale, C.G.: Turbulence modeling for time-dependent RANS and VLES: a review. AIAA J. **36**, 173–184 (1998)
29. Spalart, P.R.: Strategies for turbulence modelling and simulations. Int. J. Heat Fluid Flow **21**, 252–263 (2000)
30. Hanjalić, K.: Will RANS survive LES? A view of perspectives. J. Fluids Eng. Trans. ASME **127**, 831–839 (2005)
31. Germano, M.: Properties of the hybrid RANS/LES filter. Theor. Comput. Fluid Dyn. **17**, 225–231 (2004)
32. Kelvin, L.: On the propagation of laminar motion through a turbulently moving inviscid liquid. Philos. Mag. **24**, 342–353 (1887)
33. Chen, H., Orszag, S.A., Staroselsky, I., Succi, S.: Expanded analogy between Boltzmann kinetic theory of fluids and turbulence. J. Fluid Mech. **519**, 301–314 (2004)
34. Monin, A.S., Yaglom, A.M.: Statistical Fluid Mechanics: Mechanics of Turbulence, Vol. 1. MIT, Cambridge (1971)
35. Lebowitz, J.L., Frisch, H.L., Helfand, E.: Nonequilibrium distribution functions in a fluid. Phys. Fluids **3**, 325–338 (1960)
36. Bird, G.A.: Molecular Gas Dynamics and the Direct Simulation of Gas Flows. Clarendon, Oxford (1994)
37. Cercignani, C.: The Boltzmann Equation and its Application. Springer, Berlin Heidelberg New York (1988)
38. Alexeev, B.V.: The generalized Boltzmann equation, generalized hydrodynamic equations and their application. Philos. Trans. R. Soc. Lond. A **449**, 417–443 (1994)
39. Levermore, C.D., Morokoff, W.J., Nadiga, B.T.: Moment realizability and the validity of the Navier–Stokes equations for rarefied gas dynamics. Phys. Fluids **12**, 3214–3226 (1998)
40. Esposito, R., Lebowitz, J.L., Marra, R.: On the derivation of hydrodynamics from the Boltzmann equation. Phys. Fluids **11**, 2354–2366 (1999)
41. Heinz, S.: Nonlinear Lagrangian equations for turbulent motion and buoyancy in inhomogeneous flows. Phys. Fluids **9**, 703–716 (1997)
42. Heinz, S.: Molecular to fluid dynamics: the consequences of stochastic molecular motion. Phys. Rev. E **70**, 036308/1–11 (2004)
43. Bhatnagar, P.L., Gross, E.P., Krook, M.: A model for collision processes in gases. I. Small amplitude processes in charged and neutral one-component systems. Phys. Rev. **94**, 511–525 (1954)
44. Oldroyd, J.G.: On the formulation of rheological equations of state. Proc. R. Soc. Lond. Ser. A **200**, 523–541 (1950)
45. Tavoularis, S., Corrsin, S.: Experiments in nearly homogeneous turbulent shear flow with a uniform mean temperature gradient. Part 1. J. Fluid Mech. **104**, 311–347 (1981)
46. Schumann, U.: Realizability of Reynolds stress turbulence models. Phys. Fluids **20**, 721–725 (1977)
47. Lumley, J.L.: Computational modeling of turbulent flows. Adv. Appl. Mech. **18**, 123–175 (1978)
48. Pope, S.B.: On the relationship between stochastic Lagrangian models of turbulence and second-moment closures. Phys. Fluids **6**, 973–985 (1994)
49. Durbin, P.A., Speziale, C.G.: Realizability of second-moment closure via stochastic analysis. J. Fluid Mech. **280**, 395–407 (1994)
50. Muradoglu, M., Jenny, P., Pope, S.B., Caughey, D.A.: A consistent hybrid finite-volume/particle method for the PDF equations of turbulent reactive flows. J. Comput. Phys. **154**, 342–371 (1999)
51. Nooren, P.A., Wouters, H.A., Peeters, T.W.J., Roekaerts, D.: Monte Carlo PDF modeling of a turbulent natural-gas diffusion flame. Combust. Theory Model. **1**, 79–96 (1997)

52. Wouters, H.A., Nooren, P.A., Peeters, T.W.J., Roekaerts, D.: Simulation of a bluff-body stabilized diffusion flame using second-moment closure and Monte Carlo methods. In: Twenty-Sixth Symposium (Int.) on Combustion, pp. 177–185. The Combustion Institute, Pittsburgh (1996)
53. Yoshizawa, A., Nisizima, S., Shimomura, Y., Kobayashi, H., Matsuo, Y., Abe, H., Fujiwara, H.: A new methodology for Reynolds-averaged modeling based on the amalgamation of heuristic-modeling and turbulence-theory methods. Phys. Fluids **18**, 035109/1–17 (2006)
54. Heinz, S.: On the Kolmogorov constant in stochastic turbulence models. Phys. Fluids **14** 4095–4098 (2002)
55. Heinz, S.: A model for the reduction of the turbulent energy redistribution by compressibility. Phys. Fluids **15**, 3580–3583 (2003)
56. Haworth, D.C., Pope, S.B.: A generalized Langevin model for turbulent flows. Phys. Fluids **29**, 387–405 (1986)
57. Haworth, D.C., Pope, S.B.: A PDF modelling study of self-similar turbulent free shear flow. Phys. Fluids **30**, 1026–1044 (1987)
58. Sarkar, S.: The stabilizing effect of compressibility in turbulent shear flow. J. Fluid Mech. **282**, 163–186 (1995)
59. Moser, R.D., Kim, J., Mansour, N.N.: Direct numerical simulation of turbulent channel flow up to $Re_\tau = 590$. Phys. Fluids **11**, 943–945 (1999)
60. Delarue, B.J., Pope, S.B.: Application of PDF methods to compressible turbulent flows. Phys. Fluids **9**, 2704–2715 (1997)
61. Delarue, B.J., Pope, S.B.: Calculation of subsonic and supersonic turbulent reacting mixing layers using probability density function methods. Phys. Fluids **10**, 487–498 (1998)
62. Jones, W.P.: Launder, B.E.: The prediction of laminarization with a two-equation model for turbulence. Int. J. Heat Mass Transfer **15**, 301–314 (1972)
63. Heinz, S., Foysi, H., Friedrich, R.: A k-omega analysis of turbulent supersonic channel flow DNS data. In: Eaton, J.K., Friedrich, R., Gatski, T.B., Humphrey, J.A.C. (eds.) Proceedings of the 4th International Symposium on Turbulence and Shear Flow Phenomena, pp. 1007–1012, Williamsburg, 2005
64. Gatski, T.B., Speziale, C.G.: On explicit algebraic stress models for complex turbulent flows. J. Fluid Mech. **254**, 59–78 (1993)
65. Yoshizawa, A.: Statistical analysis of the deviation of the Reynolds stress from its eddy viscosity representation. Phys. Fluids **27**, 1377–1387 (1984)
66. Rubinstein, R., Barton, J.M.: Nonlinear Reynolds stress models and the renormalization group. Phys. Fluids **A2**, 1472–1476 (1990)
67. Speziale, C.G.: On nonlinear K-l and K-ε models for turbulence. J. Fluid Mech. **178**, 459–475 (1987)
68. Wang, D., Tong, C.: Experimental study of velocity filtered joint density function for large eddy simulation. Phys. Fluids **16**, 3599–3613 (2004)
69. Wang, D., Tong, C.: Experimental study of velocity-scalar filtered joint density function for LES of turbulent combustion. Proc. Combust. Inst. **30**, 567–574 (2005)
70. Sreenivasan, K.R.: On the universality of the Kolmogorov constant. Phys. Fluids **7**, 2778–2784 (1995)
71. Prandtl, L.: Über ein neues Formelsystem für die ausgebildete Turbulenz. Nachr. Akad. Wiss. Göttingen Math-Phys. **K1**, 6–19 (1945)
72. Lilly, D.K.: The representation of small-scale turbulence in numerical simulation of experiments. In: Goldstine, H. H. (ed.) Proceedings IBM Scientific Computing Symposium on Environmental Sciences, pp. 195–210, Yorktown Heights, New York (1967)
73. Deardorff, J.W.: Stratocumulus-capped mixed layers derived from a three-dimensional model. Boundary-Layer Meteorol. **18**, 495–527 (1980)
74. Germano, M., Piomelli, U., Moin, P., Cabot, W.H.: A dynamic subgrid-scale eddy viscosity model. Phys. Fluids **A3**, 1760–1765 (1991)
75. Lilly, D.K.: A proposed modification of the Germano subgrid-scale closure method. Phys. Fluids **A4**, 633–635 (1992)
76. Kosović, B.: Subgrid-scale modeling for the large eddy simulation of high-Reynolds number boundary layers. J. Fluid Mech. **336**, 151–182 (1997)
77. Horiuti, K.: Roles of non-aligned eigenvectors of strain-rate and subgrid-scale stress tensors in turbulence generation. J. Fluid Mech. **491**, 65–100 (2003)
78. Wang, B.C., Bergstrom, D.J.: A dynamic nonlinear subgrid-scale stress model. Phys. Fluids **17**, 035109/1–15 (2005)
79. Heinz, S.: Comment on A dynamic nonlinear subgrid-scale stress model [Phys. Fluid 17, 035109 (2005)]. Phys. Fluids **17**, 099101/1–2 (2005)
80. Wang, B.-C., Bergstrom, D.J.: Response to Comment on A dynamic nonlinear subgrid-scale stress model. Phys. Fluids 17, 099102/1–2 (2005)
81. Pope, S.B.: Stochastic Lagrangian models of velocity in inhomogeneous turbulent shear flows. Phys. Fluids **14**, 1696–1702 (2002)
82. Chapman, D.R.: Computational aerodynamics development and outlook. AIAA J. **17**, 1293–1313 (1979)
83. Baggett, J.S., Jiménez, J., Kravchenko, A.G.: Resolution requirements in large eddy simulations of shear flows. In: Annual Research Briefs, Center for Turbulence Research, NASA Ames/Stanford University, pp. 51–66 (1997)
84. Wang, M., Moin, P.: Dynamic wall modeling for large eddy simulation of complex turbulent flows. Phys. Fluids **14**, 2043–2051 (2002)